ISSN: 2963-6272, DOI: 10.11591/ehs.v2i1.pp14-29

# Meta-heuristic based power quality improvement in UPQC based grid-connected hybrid renewable energy system

## Ashish Ranjan, Jayanti Choudhary

Department of Electrical Engineering, National Institute of Technology Patna, Patna, India

# **Article Info**

#### Article history:

Received May 29, 2023 Revised Apr 23, 2024 Accepted May 1, 2024

#### Keywords:

Battery energy storage system HPSO-GWO Hybrid renewable energy system Photovoltaic Total harmonic distortion

## **ABSTRACT**

In recent days, the integration of the grid-connected load system with hybrid renewable energy system (HY-RES) to improve reliability and reduce losses are cheered. In order to satisfy the requirement of the load demand, the HY-RES is incorporated with the grid-connected load which leads to the power quality (PQ) problems in the system. Hence, the UPQC based HPSO-GWO are proposed in this paper. With the utilization of the UPQC device, the PQ issues are minimized by satisfy the load need in the HY-RES system to solve the PQ issues is the major goal of this work. To mitigate the PQ issues, the HPSO-GWO optimization algorithm with an inverter for SAPF and SH-APF is introduced to enhance the UPQC's performance. HY-RES is originally built in this study with a PV system, WT, and BESS, all of which are connected to the load system. The load is connected to the system to produce PQ difficulties in order to examine the suggested technique's presentation. With the help of the HY-RES system, PQ problems are minimized and load demand is reimbursed. The proposed method has been implemented in the MATLAB/Simulink platform, and its results have been evaluated. In this paper, for validating the performance of the proposed technique, three various cases such as sag, swell, and fluctuation is analyzed. In addition, the total harmonic distortion (THD) is analyzed. Furthermore, the suggested strategy is compared to existing methods such as GWO and PSO algorithms to prove the proposed technique is superior to existing techniques.

This is an open access article under the <u>CC BY-SA</u> license.



14

## Corresponding Author:

Ashish Ranjan

Department of Electrical Engineering, National Institute of Technology Patrna

Patna, Bihar 800005, India

Email: ashishr.phd19.ee@nitp.ac.in

## 1. INTRODUCTION

Power system (PS) networks have faced a number of challenges in the past few years including the use of fossil fuels and thermal production, which produces electricity with key emissions such as depleted fuel, pollution, and high costs [1], [2]. Renewable energy system (RES) have the potential to overcome traditional resource constraints such as pollution and global warming, [3]–[5]. To provide the stability and flexibility in the PS there is need of a global assessment of global warming, power safety, and environmental challenges. The RES is producing a high rate of increased flexibility and stability during the RES used in PS. The penetration of RES also has an impact on the stability of distribution and transmission systems [6], [7]. To ensure the maintenance of the stability, safe operation, and effective consistent operation, the system must be coordinated and monitored due to the RES causes continual development in transmission and distribution system. With RES, the system will be continuously monitored, which will increase the system's competency. Controlling power electronic devices in the PS can help the RES system run more efficiently. With RES, these controlling mechanisms improve the quality of consumers in a distributed system (DS) [8]. The usage of hybrid

research is undoubtedly affected by RES operations. A hybrid system is a collection of one or more renewable resources that are linked together in a system. To fulfill the load demands, the HY-RES can be combined with a DS. The most advanced renewable resources among the RES are PV and wind energy conversion systems (WECS). When HY-RES is coupled to distribution systems, it produces an instability situation [9]. Sag, swell, harmonics, interruptions, and disruptions, among other PQ issues, will become more prevalent in the system. The voltage level of the distribution system will oscillate due to PQ issues and causing a tripping problem. The system's reliability was harmed as a result of the emergence of continual tripping behavior [10]. By operating grid standards, the tripping problem con is recovering.

ISSN: 2963-6272

PQ concerns, like sag and voltage swell, are the most serious problem in the PS. The voltage swells and sags generate power on the consumer side by supplying minimum power from HY-RES, affecting loads and power electronic devices. To reduce these PQ difficulties, the PSs Filter and flexible AC transmission systems (FACT) devices can help [11], [12]. Numerous devices are available and divided with respect to the shunt and series devices. The voltage is compensated in a REG based PS via series devices such as DVR and SSSC. In the same way, in a PS, the shunt devices such as DSTATCOM, TCR, and STATCOM compensate the voltage [13]. By maintaining a steady voltage and injecting the required voltage level, the FACT device compensates for the PQ issues. DSTATCOM includes two control modes: one that controls the load voltage and the other that injects harmonic components and reactive in the current mode [14], [15]. The FACT device is also equipped with a critical control approach for maintaining distribution system stability. To avoid PQ problems and keep a steady condition with HY-RES-based distribution systems, adequate control is essential. Research contribution:

This research is mainly focused on mitigating PQ problems in HY-RES systems with grid-connected loads. To mitigate PQ problems in the system, the correct optimization and FACT device must be selected. The following is a summary of the main contribution of the paper:

- WT, PV, and BESS are incorporated in the HY-RES system. The WT and PV have created the power based on wind speed and irradiation levels. When WT and PV struggle to meet needed load demand due to partial shadowing and environmental factors, to store extra power and deliver needed electricity to meet load demand by BESS. The grid system is linked to the HY-RES system, and the load is connected to it.
- -PQ problems like as swell, sag, fluctuations, and harmonics can be introduced into the coupled system in both voltage and current signals. PQ difficulties have an impact on the system's stability and reliability, which can be mitigated. The UPQC device proposes the HPSO-GWO optimization-based control technique, which allows the HY-RES to minimize PQ faults and compensate for load demand.
- To balanced load requirement and receive excess energy, the controller supplied continuous electricity from the HY-RES system. The appropriate power is injected by the HY-RES to compensate the load demands and reduce the PQ issues. The two different types of controllers are created in the UPQC device such as shunt active power filter controller (SH-APF) and series active power filter controller (SAPF). By incorporating the load on the grid side, the recommended control strategy is designed and validated.
- -Three various PQ issues are examined, including sag, swell, and fluctuation, all of which are caused by applying load. In addition, harmonics are examined in two scenarios: before and after the UPQC device is connected. The proposed methodology's performance is compared to those of existing approaches such as GWO and PSO.

The paper's organizations:

This paper is consisting of the following section which is organized as follows, in section 2, the review works towards PQ mitigation are discussed. Section 3 explains the proposed system architecture and provides descriptions. In addition, this section consists of the RES in proposed design explanations, HPSO-GWO algorithm, and UPQC algorithm explanations are given. Furthermore, the result and discussion of the proposed method and comparison with existing methods are demonstrated in section 4. In section 5, the conclusion of the paper is given.

Literature review

Various researchers have used the FACT devices to alleviate PQ difficulties in this part. In this section, the PQ problem mitigation-related works are reviewed. Morshed and Fekih [16] presented WECS which is based on DFIG and a fault-tolerant control system for a hybrid PV/wind microgrid. For maintain the resilience and reduce the grid faults against the mismatched uncertainty, implements a fault-tolerant control system for the DFIG converters. The converters of PV and Wind are used as STATCOM for shared reactive power support strategies. When providing robustness against the mismatched uncertainties, the stability of the DFIG dynamics has been improved. Furthermore, the shared support strategy allowed the RES to supply required reactive power (RP) to the grid for optimizing the use of RES in the microgrid.

Liao and Milanović, [17] have discussed different compensating devices for mitigation of the PQ issues such as voltage sags, unbalance, and harmonics from their potential negative impact and mitigation effect. Some FACT devices, like as STATCOM, static VAR compensator, and DVR, have been modelled using

16 ISSN: 2963-6272

commercially available software power factory/dig silent to investigate the effects on crucial PQ concerns. The STATCOM employs two different control strategies: reactive power compensation and voltage regulation. The impact of various devices on PQ phenomena is investigated, and the results are analyzed with and without mitigation, using the proper assessment procedures.

Rajendran [18] have discussed the mitigation of PQ issues using a comparison of various control strategies. In this paper, artificial neural network (ANN), neuro-fuzzy controller (NFC), adaptive neuro-fuzzy interference system (ANFIS), and fuzzy logic controller (FLC) are the various intelligent methods. Furthermore, various optimization control techniques are utilized for the SAPF and SH-APF. Furthermore, this work was designed in the MATLAB/Simulink platform, and the proposed work's superiority was assessed by comparing it to existing approaches. The ANFIS was utilized to increase the PQ of the UPQC and reduce voltage sag and swell.

Naidu and Meikandasivam [19] have proposed the fractional order PID(FOPID) controller and PQ theory in DPFC to enhance the PQ in an HY-RES incorporated with the grid. The custom power devices (CPDs) are used in this paper to overcome PQ problems in the DS. Furthermore, to address PQ difficulties, DPFC was linked to FOPID controller and PQ theory. Against demonstrate superiority, the suggested technique FOPID was compared to FUZZY, PI, and ANFIS controllers. In addition, CPDs were used with the IEEE 12 bus system in the case study.

Al-Ammar *et al.* [20] have presented CPD based DVR power electronics which are incorporated in the DS for enhancing the PQ by mitigating the voltage sag problem. A versatile control technique based on SRF (synchronous reference frame) theory was incorporated with DVR for sensitive loads in the distribution system for balancing the voltage sag. In this paper, the fuzzy logic-based automatic switch was introduced with DVR for the detection of voltage sag. The author failed to design the DVR-based FLC and Sliding mode control (SMC) in this paper.

Liao and Milanovic [21] presented a thorough technique for assessing the techno-economics of PQ mitigation. Based on the devices, network, and optimization, PQ mitigation technique for offering differentiated PQ in-network combined with RES is proposed in this study. Because of several essential PQ occurrences, this work is based on the assessment of financial losses and the adoption of a particular diagnosis, as well as the cost of various mitigation measures and payback. Furthermore, this technique takes into account a variety of client needs and provides varying amounts of PQ across the network.

The many forms of FACT devices for mitigation of PQ problems like as voltage swell, dip, and flicker due to the rising number of nonlinear loads have been presented by Gidd *et al.* [22]. SVC, TCSC, STATCOM, DVR, UPFC, and DSTATCOM are types of FACT devices presented in this paper for power conditioning where DSTATCOM is mainly discussed here to overcome the PQ issues. The DSTATCOM modelling and its effectiveness across different loading conditions are the subject of this effort. DSTATCOM modeling and control performance are verified using MATLAB Simulink during normal operation and also when loading conditions change.

Kumar *et al.* [23] have presented PQ issues in HY-RES incorporated with grid and FACT device also interconnected. In this paper, PV, Wind, and generators are presented as energy sources. Future trends and common in RES's discussion were offered based on the maturity and reliability of each technology. The various technique was used in this paper to mitigate the PQ issues. However, there are several challenges with RES grid integration, and in light of the aforementioned tendencies, it is vital to look into potential solutions.

Soomro and Almelian [24] have presented the design of a single tuned passive filter (STPF) to limit harmonic distortion generated by nonlinear loads in a PS. It minimizes the requirement for a capacitor to provide additional kVAr. The design and implementation of the Passive filter can be discovered in various researches due to these two appealing properties. The main challenge with filter design has been a difficult one. The best design of a STPF is presented in this paper, and its application is to minimize harmonics in power frequency. Using the Lagrange interpolation approach, the best parameters of this filter were computed.

The STATCOM which is based on voltage source converter (VSC) with high bandwidth presented by Morati *et al.* [25], is meant to mitigate voltage flicker in a 100-MVA EAF installed in Europe. The addition of an active current component to the STATCOM's current reference is recommended as a novel control strategy. This control method greatly improves the STATCOM's performance in terms of voltage flicker reduction. The suggested control makes use of the VSC's DC-voltage margin to generate an active compensating current while avoiding oversizing the STATCOM converter's capacitor.

Although the solutions for mitigating PQ issues with integrated FACT devices have been successful, they do not completely solve the problem. To compensate for the PQ issues, the authors combined the coordinated PQ theory with DPFC. However, because the VSI's voltage and current grades were high in this manner, it reduced cost. To compensate for PQ difficulties, UPQC with WECS was introduced. Nonetheless, dc-link voltage maintenance was challenging with the UPQC device. For PQ difficulties, an enhanced UPQC was employed, although no active power injection was used in this technique. The majority of the issues

ISSN: 2963-6272

identified in the previous literature should be addressed by a suitable PQ issue mitigation strategy. As a result, a unique control technique will be improved and constructed with HY-RES based on the FACT device to compensate for PQ problems such as swell, voltage sag, and fluctuations, among other things.

#### 2. PROPOSED METHODOLOGY

As a result of urbanization and industrialization, the demand for utilities grows, putting more strain on the system. Because of security and power dependability issues, conventional generation sources are unable to meet today's power demand. Distributed energy (DE) RES have been employed to address these issues. The HY-RES system, the most modern technology, improves the system's efficiency and reliability.

The HY-RES system is connected to the DS to fulfil the required load demand from the consumer side, resulting in PQ issues such as stability and flexibility. Allowing the system to be more flexible and stable while eliminating PQ issues caused by the use of HY-RES in a grid-connected system. Swell, voltage sag, harmonics, and volatility are all problems that the FACT device may help with.

For similar PQ challenges in the HY-RES with grid-connected system, UPQC is proposed in this study. Figure 1 depicts the architecture of the proposed UPQC with HY-RES grid connected system. Battery, PV, and wind systems are included in the planned HY-RES that is connected to the grid in this paper. The PQ concerns at HY-RES, which is connected to the grid, developed as a result of the load. This interconnection is the source of voltage stability and reactive power mismatch issues. UPQC is the best device choice for improving voltage control in grid-connected HY-RES by reducing PQ concerns. The appropriate regulation of UPQC is improved with the use of a hybrid optimization technique known as PSO-GWO. Furthermore, with the assistance of PSO-GWO, the controlling parameters of UPQC are reached. Battery, PV and WT battery are connected with grid system which is given in Figure 1 and consumer load requirements are compensated with the help of RES. The extra electricity from PV and WT systems is stored by the battery which provides the necessary power in critical situations. The vital trouble to maintaining stability and reliability conditions in grid-connected HY-RES systems is the PQ problems. Then the PQ issues like swell, sag, and interruption are compensated by the UPQC with the grid-connected HY-RES system. With the help of control strategies in series as well as shunt filter, PQ problems are compensated by UPQC. The PSO-GWO filter is used to inject the necessary power to compensate for sag and swell. The HPSO-GWO optimization is used to optimize the gain parameters. The PV system is the optimum choice for generating power from solar energy while minimizing greenhouse gas emissions, having a long lifetime, stability with non-rotating units, little maintenance, and maximum reliability. The photovoltaic system in which cells are connected in series to get the desired voltage.

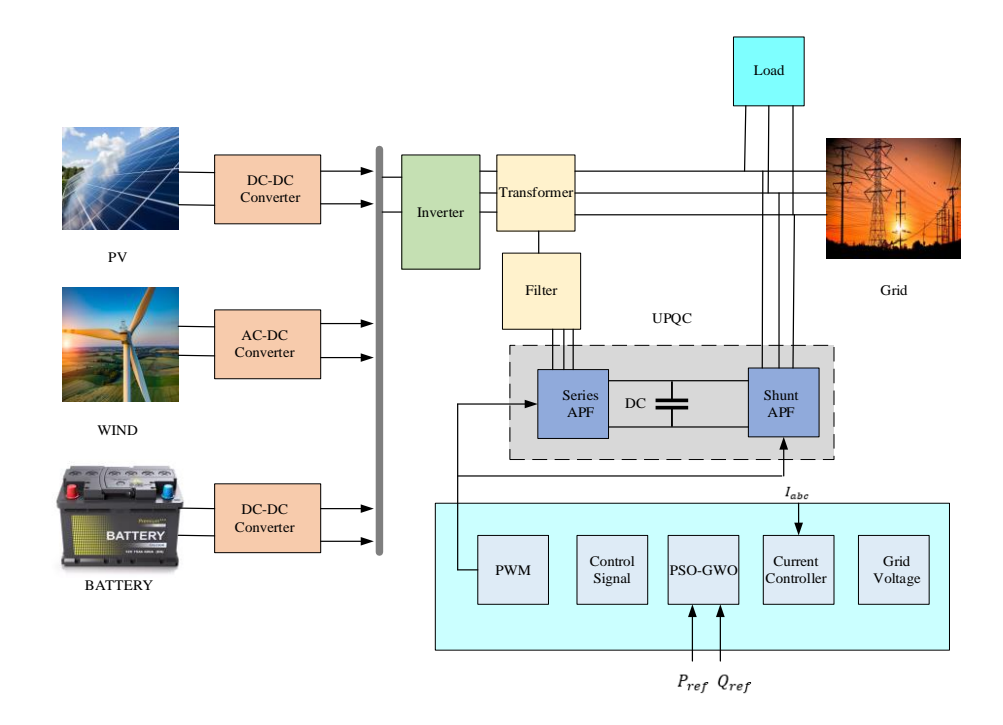


Figure 1. Structure of proposed UPQC with HY-RES grid connected system

Battery:

The battery is utilized to meet load demand when the HY-RES produces insufficient electricity. The battery range is estimated and developed based on the reference autonomy day  $(AD^*)$ , which is specified in equation, in the situation of the system's needed energy need (1).

$$Battery^{C} = \frac{AD^{*} \times p_{l}^{*}}{\eta_{l}^{*} \times \eta_{h}^{*} \times dod^{*}}$$

$$\tag{1}$$

 $AD^* = Autonomy day,$ 

 $p_l^*$  = Demand power,

 $\eta_i^*$  = Efficiency of Inverter,

 $\eta_b^*$  = Battery efficiency,

 $dod^*$  = Battery's depth of discharge rate.

The autonomy day refers to the total number of days the battery can generate enough power to meet load demand. The battery is charged with excess electricity generated by RES. As shown ini (2) illustrates the battery power.

$$B_p^* = P_{pv}^*(t) + P_{wt}^*(t) - \frac{p_l^*(t)}{\eta_l^*}$$
 (2)

 $p_l^*(t)$  = System's load demand,

 $B_n^*$  = Power of battery.

In HY-RES [26], the SOC (state of charge) is the most important battery metric that is linked to energy generation and insufficiency. As shown ini (3) demonstrates the SOC formula.

$$SOC^{*}(t) = \begin{cases} SOC^{*}(t-1)(1-\mu^{*}) + \left(P_{pv}^{*}(t) + P_{wt}^{*}(t) - \frac{p_{l}^{*}(t)}{\eta_{l}^{*}}\right) \times \eta_{b}^{*}, P_{pv}^{*}(t) + P_{wt}^{*}(t) > p_{l}^{*}(t) \\ SOC^{*}(t-1)(1-\mu^{*}) + \left(\frac{p_{l}^{*}(t)}{\eta_{l}^{*}} - P_{pv}^{*}(t) + P_{wt}^{*}(t)\right) \times \eta_{b}^{*}, P_{pv}^{*}(t) + P_{wt}^{*}(t) < p_{l}^{*}(t) \end{cases}$$
(3)

 $\mu^*$  = Battery's self-discharge rate.

Equivalent circuit of PV cell:

Several solar modules are connected in series and parallel in a PV array to define voltage, current, short circuit current (SCC), and open-circuit voltage (OCV) [27]. The equivalent circuit of the PV cell is shown in Figure 2. There are mainly three components namely current source, series resistors, and a parallel diode. Commonly, the expected power is provided from the PV cells which are assembled concurrently to make modules of PV based on the combination of series and parallel.

An  $n_s^*$  = the number of PV cells in series,

 $n_p^*$  = the number of PV cells in parallel, correspondingly. The affinity between the output current and voltage can be expressed by (4).

$$i_{pv}^* = n_p^* i_g^* - n_p^* i_s^* \left( exp \left[ \frac{Q^*}{akt_c} \left( \frac{v_{pv}^*}{n_s^*} + \frac{r_s i_{pv}^*}{n_p^*} \right) \right] - 1 \right)$$
 (4)

The generated photo current  $i_q^*$  is represented as solar irradiation, as (5).

$$i_g^* = \left(i_{sc}^* + K_i(t_c - t_{ref})\right) \frac{s}{1000}$$
 (5)

Based on the subsequent relationship,  $i_s^*$  is represented as saturation current of PV cell varies with the temperature (6).

$$i_S^* = i_{RS}^* \left[ \frac{t_C}{t_{ref}} \right]^3 exp \left[ \frac{Q^* e_g}{ak} \left( \frac{1}{t_{ref}} - \frac{1}{t_C} \right) \right]$$
 (6)

Equivalent circuit of DC-DC Converter:

The equivalent circuit of the DC-DC boost converter is shown in Figure 3. Switch sw1 is initially closed, but switch sw2 is initially open [28]. Now the inductor current L ( $I_L$ ) raising from zero. The next step

is to close switch sw2 and open switch sw1, then the inductor current goes to load, and the capacitor stores the charges. In the stable state, the ON-OFF state of the switches sw1 and sw2 are fairly be the contingent extreme

value of the output voltage  $v_o^*$ The DC-DC converter's input and output voltages with duty cycle are given in (7) to (9):

$$\frac{v_o^*}{v_{in}^*} = \frac{1}{1 - D_{duty}^*} \tag{7}$$

ISSN: 2963-6272

$$\frac{v_o^*}{v_{in}^*} = \frac{t_{rise}^*}{t_{fall}^*} + 1 \tag{8}$$

$$D_{duty}^* = \frac{t_{rise}^*}{t_{rise}^* + t_{fall}^*} \tag{9}$$

 $D_{duty}^* = \text{duty cycle},$ 

 $t_{rise}^* =$ period for raising inductor current,

switch sw1 is in closed condition.

 $t_{fall}^*$  is the time for decreasing inductor current, switch sw1 is in open condition.

Load (grid, DC load)

The  $3\varphi$  electric PS is the gold standard in ac (alternating current) generation, distribution, and transmission. It is a type of polyphase system that is, for the most part, the most widely used mechanism for transporting power in electrical grids around the world. Large motors and other large weights can also be powered using this [29]. A three-wire  $3\varphi$  circuit is more cost-effective than a two-wire single- $\varphi$  equivalent circuit on the same transmission line to ground voltage because it needs less material for the conductor to transfer a certain quantity of electrical power. After the PQ has been boosted and the loss has been compensated, the energy is stored in the grid for subsequent consumption. The transmission line is used to send power to both three-phase loads and the grid. As a result, the proposed methodology was used to achieve effective power compensation.

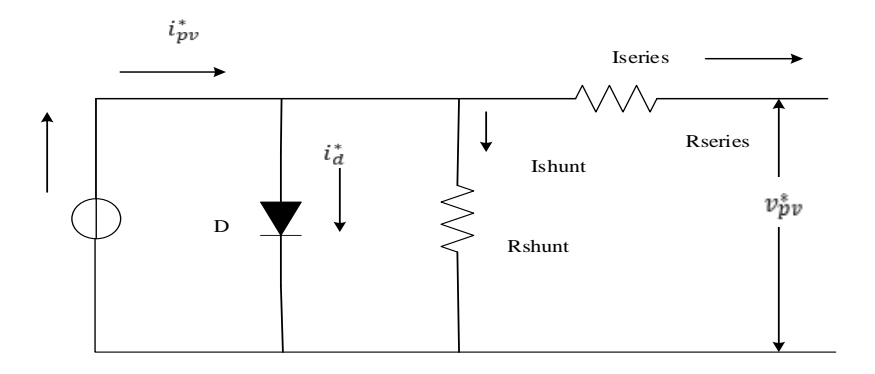


Figure 2. PV cell equivalent circuit

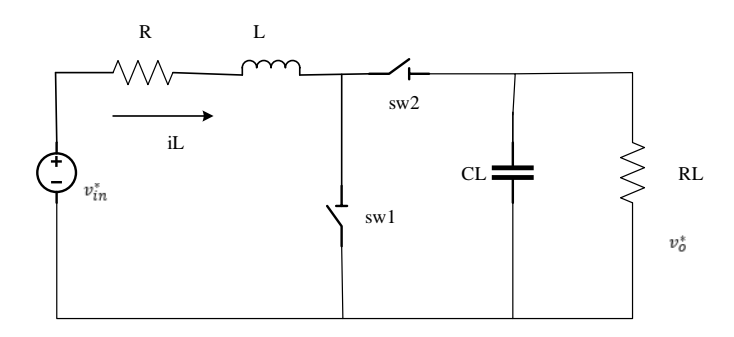


Figure 3. Equivalent circuit of DC-DC boost converter

20 ISSN: 2963-6272

# 2.1. Control strategy of UPQC

UPQC mainly depends on the SH-APF and SAPF controllers are responsible for the majority of UPQC's whole function. A HPSO-GWO optimization algorithm-based PI controller is suggested for PQ correction. A SAPF has a high impedance for current harmonics, blocks load headings and source streams, and supplies voltage as a voltage supply in time. The primary goal of series compensators is to eliminate the harmonic mechanism in the voltage supply [30].

SAPF the rated voltage and load bus sine curve are tracked by the UPQC's SAPF. As a result, the simplest method is to directly load the voltage of load bus sine curve to prepare a series of converters including matching motions. In a typical home, for example, single-phase 230-volt AC/ 50 Hz energy with a fixed power output is used. At fixed range of load voltage, the sine curve voltage sensitivity is therefore safeguarded at fundamental frequency (e.g., 50 Hz), and (ii) for proper load, the two basic factors are expressly rated to offer accurate load bus control. As a result of unwanted occurrences, the power supply voltage may be twisted in a comparable feeder, such as capacitor bank, a high-frequency load is turning on/off, and so on, generating droop or voltage spikes. If the fixed of sine curve voltage and the critical voltage of load, the range of load voltage may be undesirable and recognized problems or events can be removed easily. This is the voltage required for the state to create a perfect sine curve voltage when the prescribed range has been reached, allowing the SAPF to be changed and the power voltage distortion to be eliminated. In other words, a series of filters transform the voltage applied by the power to the appropriate voltage. The controller for the series APF in UPQC is shown in Figure 4.

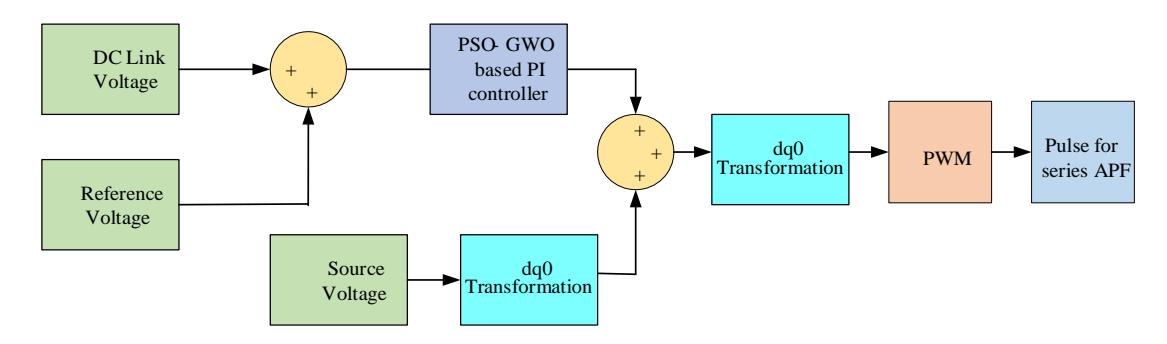


Figure 4. Control structure for series APF

SH-APF to construct a reference current signal for the SH-APF, the unit vector template is employed. The SH-APF's main function is to maintain a steady DC voltage, which aids current synchronization and reactive power. Compressing the source current sinusoidal wave is the simplest way to compensate for the aforementioned load issues. Figure 5 depicts the APF shunt controller in UPQC.

A fault was injected into the transmission line to test the power adjustment. This method tests and evaluates the suggested technique's power stability. Finally, the defects are eliminated utilizing the above-mentioned proposed mechanism, which utilizes a UPQC controller with a PSO-GWO-based PI controller. Once the faults and distortions are corrected, the stabilized electricity is stored in a three-phase grid.

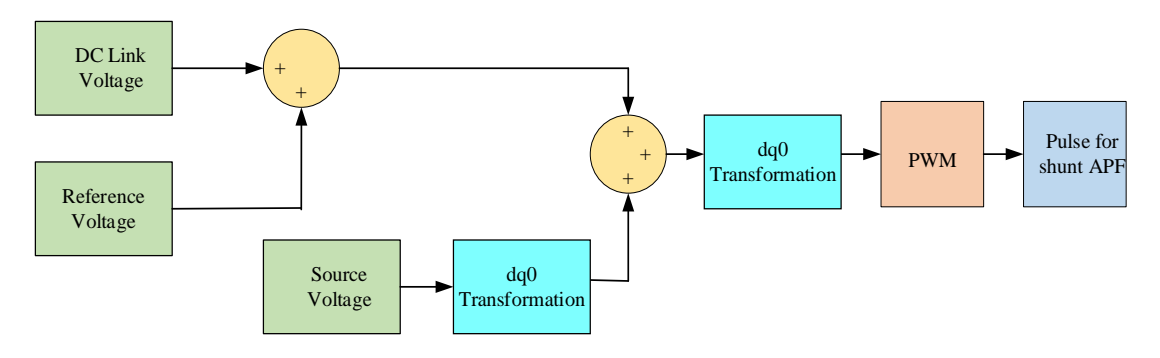


Figure 5. Control structure for shunt APF

# 2.2. Background of PSO and GWO techniques

The gain parameters such as  $k_p$  and  $k_i$  are the parameters of PI controller of UPQC, which is regulate for reducing the steady state error, rise time, overshoot and eliminate the error. The PSO-GWO is used to determine the PI's best parameters.

-PSO

The PSO is one of the most basic and widely used optimization methods. Through this technique, a number of particles are allowed to move in a multidimensional search space. The velocity of each particle must be updated while searching [31].

$$V_j^{K+1} = \omega^* V_j^K + c_1^* rand_1^* \left( p_{j,pbest}^K - X_j^K \right) + c_2^* rand_2^* \left( p_{j,qbest}^K - X_j^K \right)$$
 (10)

 $\omega^*$  = Initial Weight, range between 0.4 to 0.9,

 $rand_1^*$  and  $rand_2^*$  = random variables in between 0 to 1,

 $c_1^*$  and  $c_2^*$  = acceleration coefficient.

The position of swarm is updated by (11):

$$X_i^{NEW} = X_i^* + V_i^* \tag{11}$$

The most excellent solution can be obtained with more iteration is given by (12):

$$X_j^{K+1} = \left\{ \frac{X_{j,NEW}^* \quad if \quad F(X_{j,NEW}^*) \le F(X_j^*)}{X_j^* \quad otherwise} \right\}$$
 (12)

- Grey wolf optimization (GWO)

The GWO is a new metaheuristic technique based on swarm intelligence that is inspired by grey wolf hunting mindset. Grey wolves are placed in a spot and remain as a pack to carry out the hunting activity. To mathematically describe the hunting process, the best fittest answer is given to the  $\alpha^*$  group of wolves, who are then followed by the  $\beta^*$ ,  $\gamma^*$ , and  $\delta^*$  groups [32]. The wolves perform a loop around the victim during the first phase of hunting. The (13) and (14):

$$\overrightarrow{D_*} = |\overrightarrow{C_*}.\overrightarrow{X_{p*}}(t) - \overrightarrow{X_*}(t)| \tag{13}$$

$$\overrightarrow{X_*}(t+1) = \left| \overrightarrow{X_{p*}}(t) - \overrightarrow{A_*} \cdot \overrightarrow{D_*} \right| \tag{14}$$

t = Current iteration,

 $X_* = \text{Grey wolf},$ 

 $X_{n*}$  = Victim position,

 $A_*$  and  $C_*$  = Coefficient vectors

$$\overrightarrow{A_*} = 2. \overrightarrow{a_*}. \overrightarrow{r_1} - \overrightarrow{a_*} \tag{15}$$

$$\overrightarrow{C_*} = 2.\overrightarrow{r_2} \tag{16}$$

 $r_1$  and  $r_2$  = Random vectors in between 0 to 1,

During the iteration,  $a_*$  decreases from 2 to 0. The process of hunting can be formulated as (17) and (18):

$$\overrightarrow{D_{\alpha^*}^*} = \left| \overrightarrow{C_1^*} . \overrightarrow{X_{\alpha^*}^*} - \overrightarrow{X^*} \right| , \overrightarrow{D_{\beta^*}^*} = \left| \overrightarrow{C_2^*} . \overrightarrow{X_{\beta^*}^*} - \overrightarrow{X^*} \right| , \overrightarrow{D_{\delta^*}^*} = \left| \overrightarrow{C_3^*} . \overrightarrow{X_{\delta^*}^*} - \overrightarrow{X^*} \right|$$

$$(17)$$

$$\overrightarrow{X_1^*} = \overrightarrow{X_{\sigma^*}^*} - \overrightarrow{A_1^*}.(\overrightarrow{D_{\sigma^*}^*}), \overrightarrow{X_2^*} = \overrightarrow{X_{\sigma^*}^*} - \overrightarrow{A_2^*}.(\overrightarrow{D_{\sigma^*}^*}), \overrightarrow{X_3^*} = \overrightarrow{X_{\delta^*}^*} - \overrightarrow{A_3^*}.(\overrightarrow{D_{\delta^*}^*})$$

$$(18)$$

The most excellent position of prey is found by the average value of positions of  $\alpha^*$ ,  $\beta^*$  and  $\delta^*$ wolves which is given as (19):

$$\overrightarrow{X_*}(t+1) = \frac{\overrightarrow{X_1^*} + \overrightarrow{X_2^*} + \overrightarrow{X_3^*}}{3} \tag{19}$$

-HPSO-GWO

When confronted with a severe constraint, the PSO technique has the drawback of getting stuck in local minima; yet, it has some advantages, such as simplicity, robustness, and ease of implementation. GWO, on the other hand, avoids becoming stranded in one location and maintains a healthy mix of exploration and

exploitation. The HPSO-GWO algorithm thus incorporates both of these exceptional qualities of PSO and GWO.

#### Operation of PSO:

Step 1: Determine each particle's fitness function.

Step 2: Compute the global gbest and the individual pbest.

Step 3: As shown in (10) is used to keep track of swarm velocity.

Step 4: As shown in (11) is used to update the position of the swarm.

Step 5: Determine each particle's fitness values.

Step 6: The optimal solution is chosen for the next iteration based on a comparison of each particle's fitness value (12).

# Operation of GWO:

Step 7: The final population of the PSO is the initial population of GWO

Step 8: The parameter  $A_*$ ,  $C_*$  and  $a_*$  are updated using (15) and (16).

Step 9: For each search agent, random position is generated.

Step 10: The grey wolves' fitness levels are calculated using the objective function.

Step 11: Updating the parameters and position of grey wolves.

Step 12: By comparing the fitness functions, best solution is chosen for next iteration.

Step 13: The optimal solution for subsequent iteration is chosen by comparing fitness functions.

Step 14:  $X_{\alpha^*}^*$ ,  $X_{\beta^*}^*$  and  $X_{\delta^*}^*$  are updated.

Step 15: The aforementioned step is repeated until the halting requirement is met.

Step 16: The optimal controller parameters are finally obtained.

The below flowchart shows the PSO-GWO.

Including swell, sag, and voltage fluctuation using the current, voltage, and fault situations with THD, with the help of proposed controller the HY-RES with grid-connected system is estimated. Simulink is used to implement the proposed method. The proposed technique is compared to GWO and PSO techniques that are already in use Figure 6. Table 1 demonstrates the parameters of the Simulink.

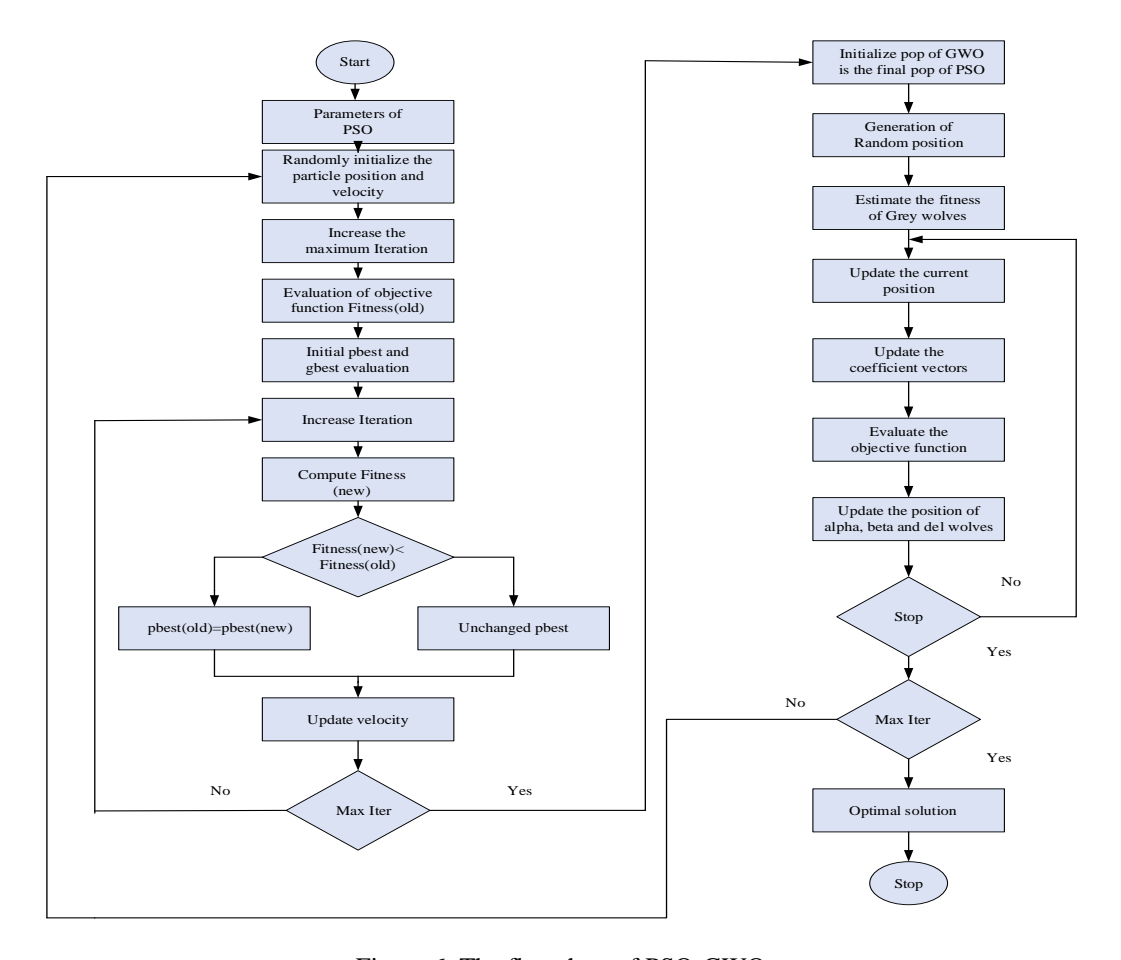


Figure 6. The flowchart of PSO-GWO

Table 1. Parameters of simulation			
S. No	Description	Parameters	Values
1	PV	Irradiance	1000 wb/m2
		Temperature	25 deg Celsius
2	Wind	Base wind speed	12m/s
		Base Rotational speed	1m/s
		Nominal mechanical output power	8.5 KW
		Stator phase resistance	0.425 ohm
3	Battery	Type	Lithium Ion
		Nominal voltage	440 V
		Initial SOC	100 %
4	Grid	Phase voltage	600 V
		Frequency	60 Hz
5	Load	Nominal voltage	100 KV
		Nominal frequency	60 Hz
		Active power	250 KW
6	PSO-GWO	Maximum iteration	500
		Number of Search agents	30

Table 1 Parameters of simulation

ISSN: 2963-6272

## 3. METHOD

The proposed method is estimated in the system by introducing PQ issues such as swell, sag, and voltage variation. The calculation of proposed design structure under three types of fault conditions: swell, sag, voltage fluctuation, and error signal levels in the system. The system performance is analyzed using three different cases, which are described below. Figure 7 demonstrates the Simulink diagram of the proposed structure without UPQC.

Figure 8 demonstrates the structure of the proposed Simulink model with UPQC. Initially, the HY-RES are linked at the source side, followed by grid and load connections at the load side, and finally, the UPQC is connected via the transformer and filter.

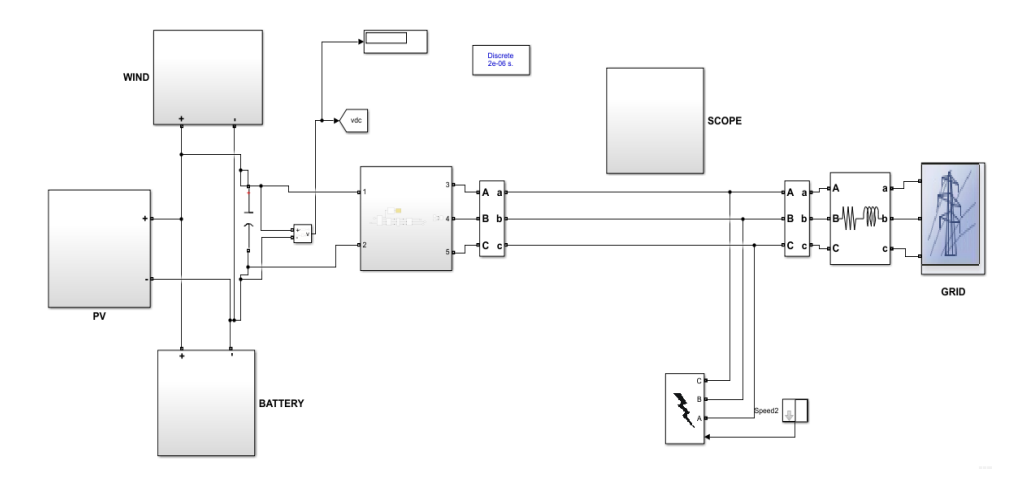


Figure 7. The proposed structure of the Simulink without UPQC

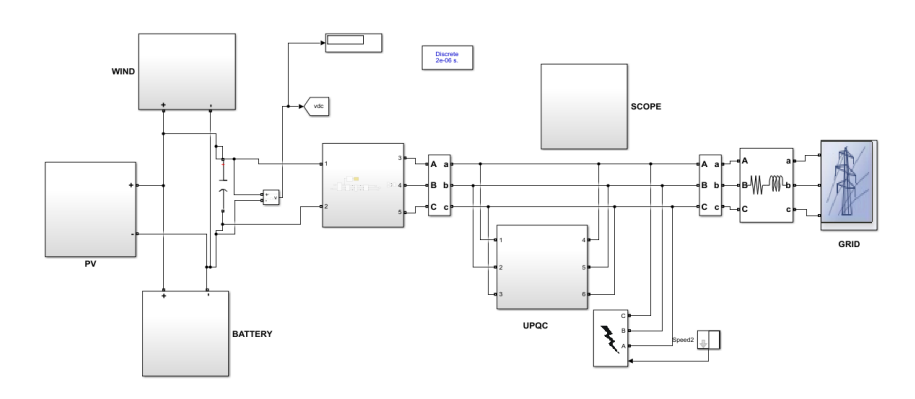


Figure 8. The proposed structure of the Simulink with UPQC

24 □ ISSN: 2963-6272

#### 4. RESULT AND DISCUSSION

The irradiance and temperature of the PV is given as 1000 wb/m2 and 25 degrees Celsius. Figure 9 illustrates the outcomes of one of the RES which is the PV. This figure demonstrates the voltage, current and power of the PV. The generated voltage of the PV is 200 V and attain the steady state in 0.1 sec and current is 312 A and power of the PV is 60 KW.

Wind voltage, current and power of that is illustrated in the Figure 10. Voltage of the wind turbine attain 130 V at 0.1 sec, current generated by the wind is 50 A and power of the wind is 6 KW at 0.1 sec. The wind speed, rotor speed, generator torque, and pitch angle of the wind turbine are all depicted in Figure 11. The wind speed varies from 12 to 15 m/s depending on the direction of the wind, the rotor speed is 1500 rpm, the torque is 3.5 N/m, and the wind turbine pitch angle is zero to one. In Simulink, the base wind speed is set to 12 m/s, the base rotational speed is set to 1 m/s, the nominal mechanical output power is 8.5 KW, and the stator phase resistance is 0.425 ohm.

Furthermore, parameters of the battery are given in the Table 1, in this work, the lithium-Ion type battery is selected. Then nominal voltage of that battery is 440 V and initial (SOC) value id set as 100% then it will be discharging condition. From Figure 12 voltage of the battery generated in the Simulink 250 V attained at 0.1sec which is in discharging condition. Then current of the battery reached 1150A at 0.1sec. Finally given the SOC which is decreasing from 100%. Figure 13 shows the analysis of the DC link voltage. The DC link voltage is attained steady state voltage 225V at 0.1 sec. This DC link capacitor is connected in between the series APF and Shunt APF of UPQC.

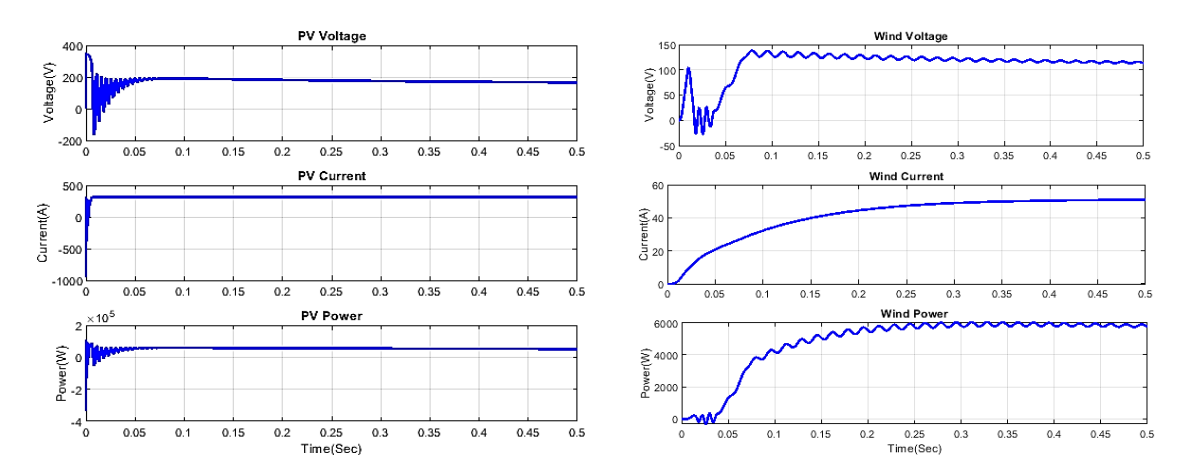


Figure 9. Analysis of PV voltage, current and power

Figure 10. Analysis of wind voltage, current and power

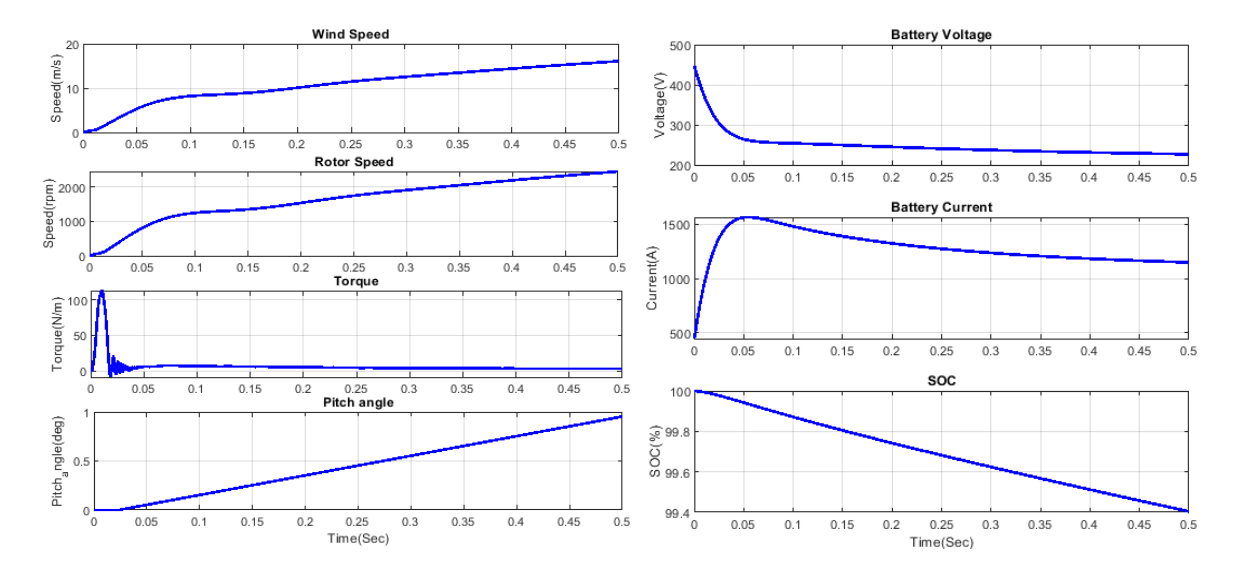


Figure 11. Analysis of wind speed, rotor speed, torque and pitch angle

Figure 12. Analysis of battery voltage, current and SOC

Figure 14 demonstrates the analysis of converter input voltage, current and output voltage. This converter is incorporated after the PV for boosting purpose and converter the dc signal into dc for inverter. The input voltage of the converter attained steady state voltage 200 V at 0.1 sec, current of the converter is 300 A and output voltage of the converter is attained steady state voltage 265 V at 0.1 sec.

# -Case 1: sag mitigation

Adding a load to the HY-RES with a grid-connected system causes sag faults in the system during this time, and the PV irradiance is set at 1000 wb/m2 in this scenario. To satisfy the demand of load, the system produce the energy based on the amount of PV irradiation; the WT speed is set to 12 m/s depending on the rate at which the WT generated the power. As a result, HY-RES was able to match the load demand while also adjusting for PQ issues. The battery in a PV or WT energy storage system can only be used in certain scenarios. In order for the system to perform linearly and consistently, the voltage sag must be resolved. The UPQC is used to ensure that adequate power is delivered to meet load requirements while avoiding PQ issues.

The study of the voltage sag situation (source voltage, load voltage, and injection current) is shown in Figure 15. In this figure source voltage is attained 455 V, from the time interval 0.15 sec to 0.3 sec the sag signal is created and then the injected current is given by the UPQC to compensated the sag signal to blunt the PQ issues. The final graph shows the load or compensated voltage. From 0.15 sec to 0.3 sec that sag signal compensated in the load voltage.

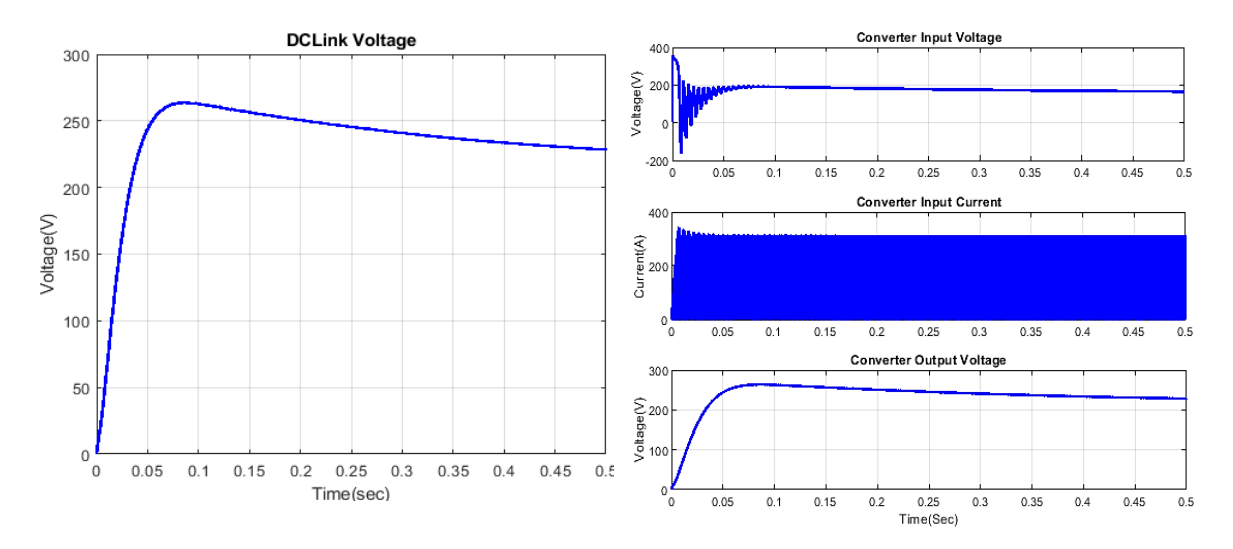


Figure 13. Analysis of DC link voltage

Figure 14. Analysis of converter input voltage, current and output voltage

# -Case 2: swell mitigation

The proposed methodology's performance is evaluated using the swell condition. By connecting the load with fault, swell conditions are formed in the system. Sources are diversified and performances are analyzed in this swell condition analysis. The WT speed and PV irradiance conditions are changed, and the effects of voltage and current swell on PQ are investigated.

Figure 16 shows the survey of voltage swell condition supply voltage, injection current and load voltage. The swell signal created in the source side from the particular time interval 0.15 sec to 0.3 sec. Then the UPQC injected current is given to compensate the source signal from the interval 0.15 sec to 0.3 sec. Further last graph shows the compensated load voltage.

# -Case 3: Fluctuation mitigation

The system's performance is assessed in this scenario under fluctuation conditions, which are caused by a load with a failure in the HY-RES. Source voltage, injection current, and load voltage are all analyzed in Figure 17. In source voltage, the voltage of source side attained 455 V and the fluctuation is created in between the time interval 0.15 sec to 0.3 sec. Then the injected current used to compensate by the UPQC which 0.2 A from 0 to 0.15 sec after 0.15 sec it will be raised and fluctuate till the 0.3 sec. This injects current compensate the load side voltage. However, the load voltage reaches steady voltage which is 455 V. Analysis of comparison:

The proposed methodology is evaluated using a comparison study under a variety of sag, swell, and voltage fluctuation situations. The HY-RES system's actual and reactive power can be compared to existing

26 □ ISSN: 2963-6272

PSO and GWO algorithms. The signals' harmonics were also investigated and validated, both with and without UPQC. The comparison is taken for the sag mitigation of proposed with the existing of PSO and GWO algorithm in Figure 18. In Figure 18, the proposed method is reached 455 V and then the time duration from 0.15 sec to 0.3 sec the sag issue is mitigated. The mitigation of the proposed voltage is better than the other techniques such as PSO and GWO. Figure 18 demonstrates the comparison of the sag mitigation. Where blue color line which is denoted the proposed work, the pink line denoted the GWO and green line denoted the PSO. In addition, the particular mitigation part is magnified to confirm the difference between the proposed and existing work.

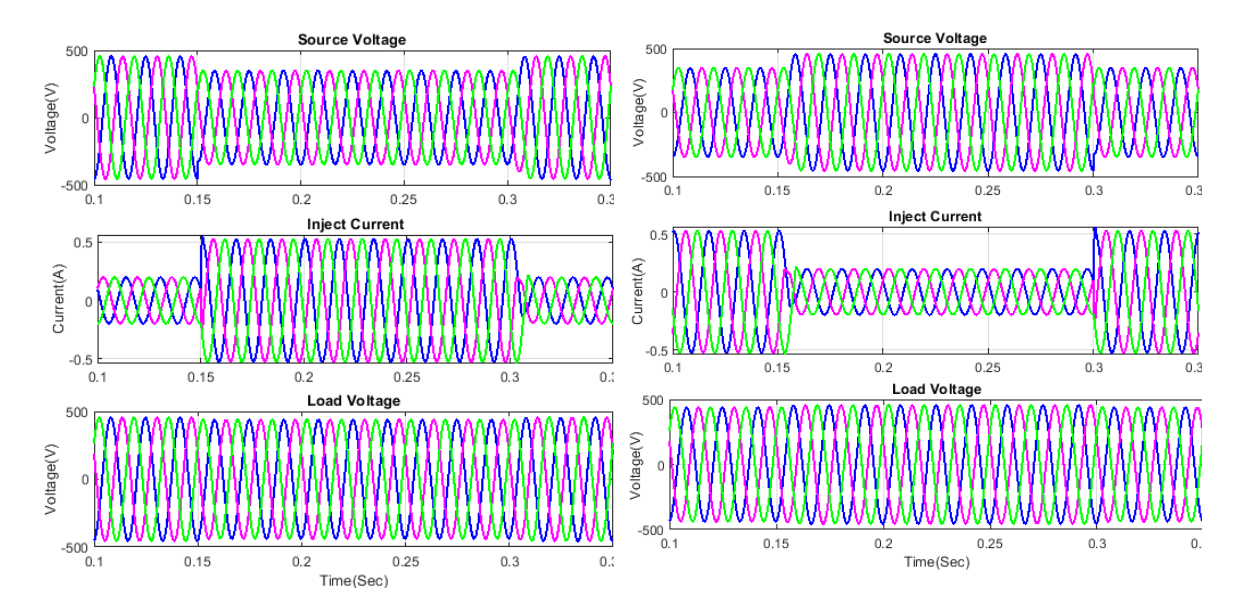


Figure 15. Survey of voltage sag condition source voltage, injection current and load voltage

Figure 16. Voltage determination source voltage, injection current, and load voltage under swell conditions

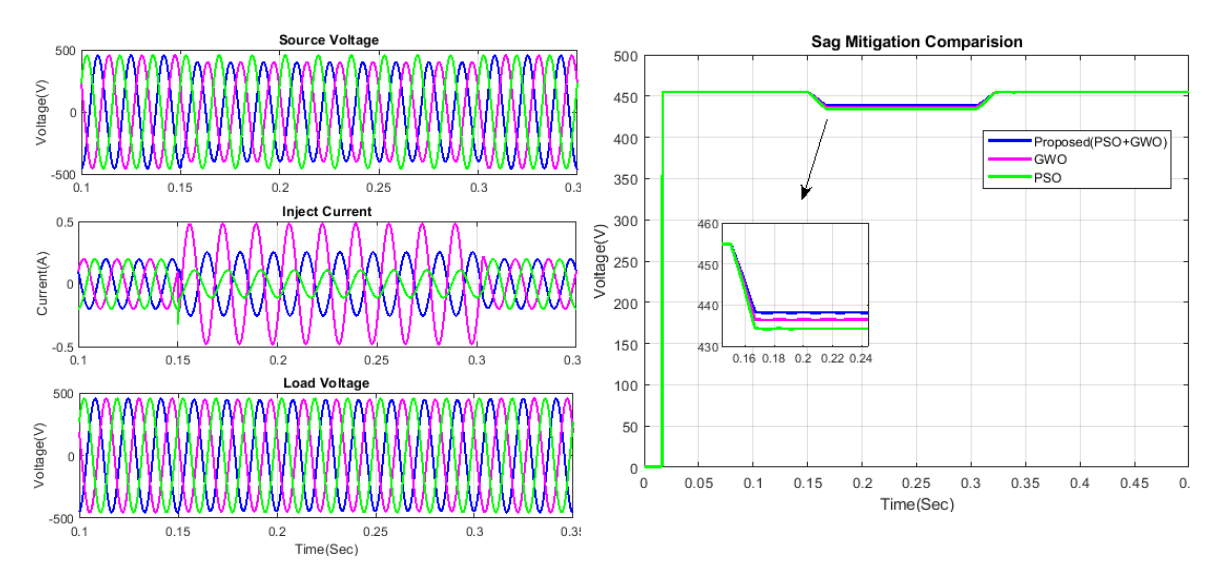


Figure 17. Source voltage, injection current, and load voltage fluctuation analysis

Figure 18. Comparison of voltage sag condition

Figure 19 demonstrates the comparison of the swell mitigation. The fact that the suggested approach outperforms the PSO and GWO is evident from this graph. Unlike the PSO and GWO, the swell signal is considerably reduced. Therefore, the proposed line is below the PSO and GWO. Here also blue line shows the

proposed technique, pink and green shows the PSO and GWO respectively. Furthermore, particular time interval is magnified to see the superior of the proposed technique. Figure 20 illustrates the comparison of the fluctuation mitigation. The fact that the suggested approach outperforms the PSO and GWO is evident from this graph. Compared to the PSO and GWO, the fluctuation signal is considerably reduced. Therefore, the proposed line is above the PSO and GWO. Here also blue line shows the proposed technique, pink and green shows the PSO and GWO respectively. Furthermore, particular time interval is magnified to see the superior of the proposed technique.

Figures 21 and 22 demonstrates the THD of the proposed technique with and without UPQC. Figure 21 shows the THD of the proposed technique without UPQC. In this figure the harmonic mitigation is 3.28% only, in Figure 22, With respect to the frequency in Hz, the total harmonic mitigation value is 0.01 percent. Furthermore, it is well known that the suggested UPQC with HPSO-GWO technique outperforms the existing PSO and GWO strategies. The PQ issues mitigated greatly by this UPQC with PSO-GWO techniques.

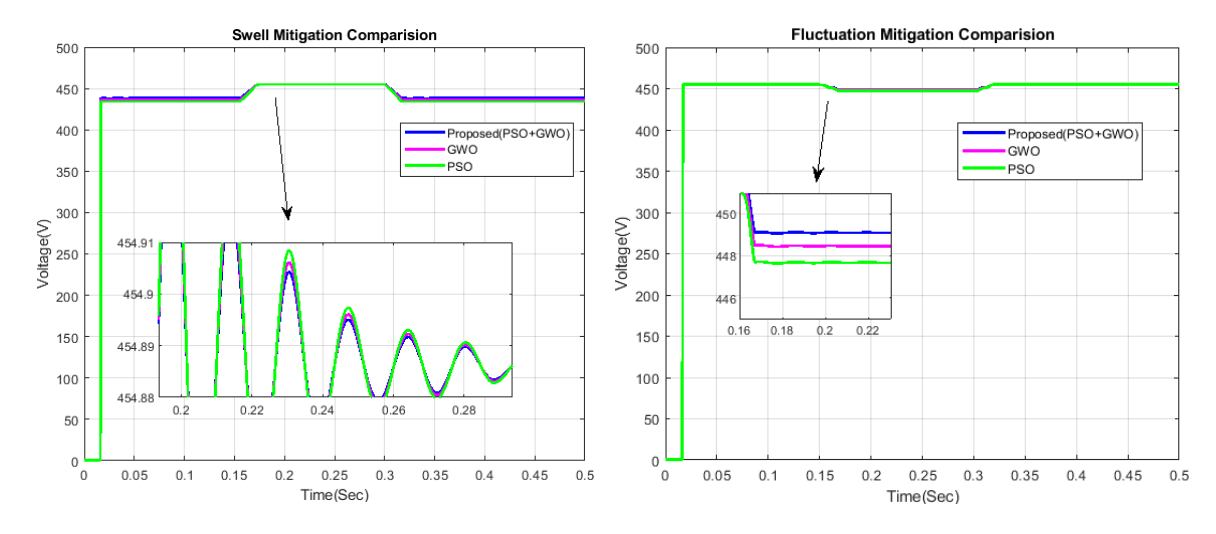


Figure 19. Comparison of voltage swell condition

Figure 20. Comparison of voltage fluctuation condition

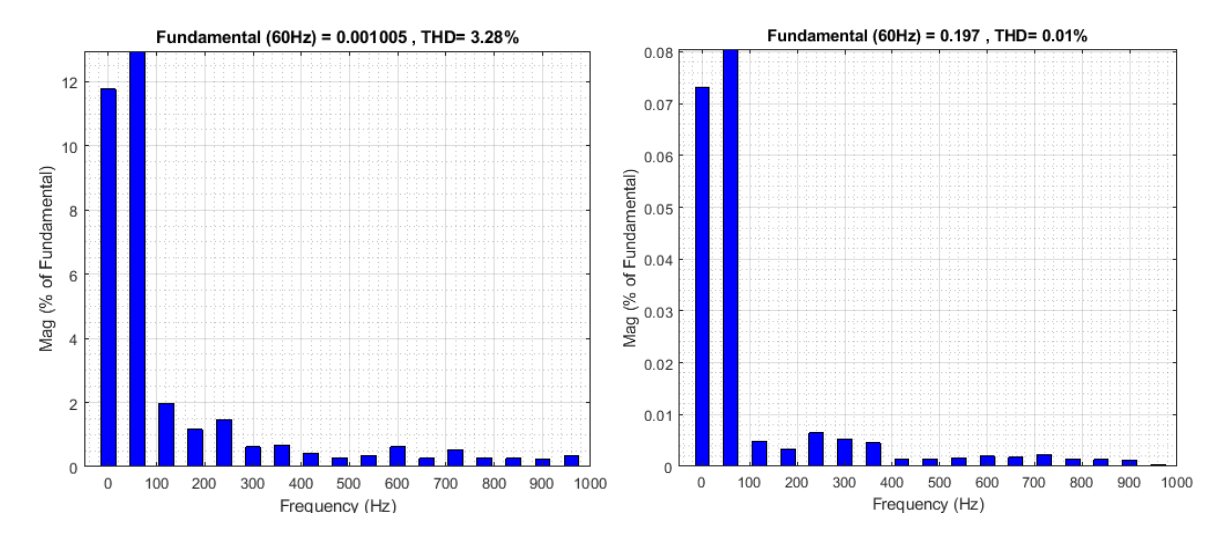


Figure 21. THD without UPQC

Figure 22. THD with UPQC

## 5. CONCLUSION

In grid-connected PS, PQ mitigation in HY-RES has become an attractive topic of analysis. The employment of load and high frequency switching characteristics on the output side has an impact on the PQ in an HY-RES, PS. As a result, to solve PQ concerns, FACT devices have been integrated into the system. To reduce the PQ concerns and satisfy the demand of load, an appropriate controller with the HY-RES and UPQC. PV, WT, and BESS systems are used in the proposed HY-RES system. Under certain environmental conditions,

ISSN: 2963-6272 28

the BESS system is utilized to adjust load demand. Two controllers make up the UPQC: an SAPF and an SH-APF, with a parameter adjustment PI controller with PSO-GWO. The suggested UPQC system addresses the voltage-related PQ issues. In MATLAB/Simulink, the proposed method is simulated and implemented. Voltage sag, swell, fluctuation, and harmonics are used to evaluate the system's results. Finally, the suggested strategy is compared to existing optimization-based controllers such as PSO and GWO.

#### REFERENCES

- I. Tlili, "Renewable energy in Saudi Arabia: current status and future potentials," Environment, Development and Sustainability, vol. 17, no. 4, pp. 859–886, Aug. 2015, doi: 10.1007/s10668-014-9579-9.
- B. N. Stram, "Key challenges to expanding renewable energy," Energy Policy, vol. 96, pp. 728-734, Sep. 2016, doi: 10.1016/j.enpol.2016.05.034.
- G. Papaefthymiou and K. Dragoon, "Towards 100% renewable energy systems: Uncapping power system flexibility," Energy Policy, vol. 92, pp. 69-82, May 2016, doi: 10.1016/j.enpol.2016.01.025.
- I. Colak, E. Kabalci, G. Fulli, and S. Lazarou, "A survey on the contributions of power electronics to smart grid systems," Renewable and Sustainable Energy Reviews, vol. 47, pp. 562-579, Jul. 2015, doi: 10.1016/j.rser.2015.03.031.
- M. R. Elkadeem, S. Wang, S. W. Sharshir, and E. G. Atia, "Feasibility analysis and techno-economic design of grid-isolated hybrid renewable energy system for electrification of agriculture and irrigation area: A case study in Dongola, Sudan," Energy Conversion and Management, vol. 196, pp. 1453-1478, Sep. 2019, doi: 10.1016/j.enconman.2019.06.085.
- J. Sun et al., "Renewable energy transmission by HVDC across the continent: system challenges and opportunities," CSEE Journal of Power and Energy Systems, vol. 3, no. 4, pp. 353-364, Dec. 2017, doi: 10.17775/CSEEJPES.2017.01200.
- F. H. Gandoman et al., "Review of FACTS technologies and applications for power quality in smart grids with renewable energy systems," Renewable and Sustainable Energy Reviews, vol. 82, pp. 502-514, Feb. 2018, doi: 10.1016/j.rser.2017.09.062
- W. U. K. Tareen et al., "Mitigation of power quality issues due to high penetration of renewable energy sources in electric grid [8] systems using three-phase APF/STATCOM technologies: a review," Energies, vol. 11, no. 6, Jun. 2018, doi: 10.3390/en11061491.
- K. Jeyaraj, D. Durairaj, and A. I. S. Velusamy, "Development and performance analysis of PSO-optimized sliding mode controllerbased dynamic voltage restorer for power quality enhancement," International Transactions on Electrical Energy Systems, vol. 30, no. 3, Mar. 2020, doi: 10.1002/2050-7038.12243.
- K. Sayahi, A. Kadri, F. Bacha, and H. Marzougui, "Implementation of a D-STATCOM control strategy based on direct power control method for grid connected wind turbine," International Journal of Electrical Power & Energy Systems, vol. 121, Oct. 2020, doi: 10.1016/j.ijepes.2020.106105.
- [11] A. H. Elmetwaly, A. A. Eldesouky, and A. A. Sallam, "An adaptive D-FACTS for power quality enhancement in an isolated microgrid," IEEE Access, vol. 8, pp. 57923-57942, 2020, doi: 10.1109/ACCESS.2020.2981444.
- [12] E. Hossain, M. R. Tur, S. Padmanaban, S. Ay, and I. Khan, "Analysis and mitigation of power quality issues in distributed generation
- systems using custom power devices," *IEEE Access*, vol. 6, pp. 16816–16833, 2018, doi: 10.1109/ACCESS.2018.2814981.

  M. Barghi Latran, A. Teke, and Y. Yoldaş, "Mitigation of power quality problems using distribution static synchronous compensator: a comprehensive review," IET Power Electronics, vol. 8, no. 7, pp. 1312-1328, Jul. 2015, doi: 10.1049/ietpel.2014.0531
- [14] D. De Yong, S. Bhowmik, and F. Magnago, "An effective power quality classifier using wavelet transform and support vector machines," Expert Systems with Applications, vol. 42, no. 15-16, pp. 6075-6081, Sep. 2015, doi: 10.1016/j.eswa.2015.04.002.
- X. Liang, "Emerging power quality challenges due to integration of renewable energy sources," IEEE Transactions on Industry Applications, vol. 53, no. 2, pp. 855–866, Mar. 2017, doi: 10.1109/TIA.2016.2626253.
- M. J. Morshed and A. Fekih, "A novel fault ride through scheme for hybrid wind/PV power generation systems," IEEE Transactions on Sustainable Energy, vol. 11, no. 4, pp. 2427-2436, Oct. 2020, doi: 10.1109/TSTE.2019.2958918.
- [17] H. Liao and J. V. Milanović, "On capability of different FACTS devices to mitigate a range of power quality phenomena," IET Generation, Transmission & Distribution, vol. 11, no. 5, pp. 1202-1211, Mar. 2017, doi: 10.1049/iet-gtd.2016.1017.
- M. Rajendran, "Comparison of various control strategies for UPQC to mitigate PQ issues," Journal of The Institution of Engineers (India): Series B, vol. 102, no. 1, pp. 19-29, Feb. 2021, doi: 10.1007/s40031-020-00502-4.
- R. Pavan Kumar Naidu and S. Meikandasivam, "Power quality enhancement in a grid-connected hybrid system with coordinated PQ theory & fractional order PID controller in DPFC," Sustainable Energy, Grids and Networks, vol. 21, p. 100317, Mar. 2020, doi: 10.1016/j.segan.2020.100317.
- E. A. Al-Ammar, A. Ul-Haq, A. Iqbal, M. Jalal, and A. Anjum, "SRF based versatile control technique for DVR to mitigate voltage sag problem in distribution system," Ain Shams Engineering Journal, vol. 11, no. 1, pp. 99-108, Mar. 2020, doi: 10.1016/j.asej.2019.09.001.
- H. Liao and J. V. Milanović, "Techno-economic analysis of global power quality mitigation strategy for provision of differentiated quality of supply," International Journal of Electrical Power & Energy Systems, vol. 107, pp. 159-166, May 2019, doi: 10.1016/j.ijepes.2018.11.006.
- A. R. Gidd, A. D. Gore, S. B. Jondhale, O. V. Kadekar, and M. P. Thakre, "Modelling, analysis and performance of a DSTATCOM for voltage sag mitigation in distribution network," in 2019 3rd International Conference on Trends in Electronics and Informatics (ICOEI), Apr. 2019, pp. 366-371, doi: 10.1109/ICOEI.2019.8862554.
- V. Kumar, A. S. Pandey, and S. K. Sinha, "Grid integration and power quality issues of wind and solar energy system: A review," in 2016 International Conference on Emerging Trends in Electrical Electronics & Sustainable Energy Systems (ICETEESES), Mar. 2016, pp. 71-80, doi: 10.1109/ICETEESES.2016.7581355.
- D. M. Soomro and M. Almelian, "Optimal design of a single tuned passive filter to mitigate harmonics in power frequency," ARPN Journal of Engineering and Applied Sciences, vol. 10, no. 19, pp. 9009-9014, 2015.
- M. Morati, D. Girod, F. Terrien, V. Peron, P. Poure, and S. Saadate, "Industrial 100-MVA EAF voltage flicker mitigation using VSC-Based STATCOM with improved performance," IEEE Transactions on Power Delivery, vol. 31, no. 6, pp. 2494–2501, Dec. 2016, doi: 10.1109/TPWRD.2015.2508498.
- O. P. Mahela and A. G. Shaik, "Power quality improvement in distribution network using DSTATCOM with battery energy storage system," International Journal of Electrical Power & Energy Systems, vol. 83, pp. 229-240, Dec. 2016, doi: 10.1016/j.ijepes.2016.04.011.
- V. Tamrakar, S. C. Gupta, and Y. Sawle, "Study of characteristics of single and double diode electrical equivalent circuit models

of solar PV module," in 2015 International Conference on Energy Systems and Applications, Oct. 2015, pp. 312–317, doi: 10.1109/ICESA.2015.7503362.

ISSN: 2963-6272

- [28] S. Bhat and I. R. Ballal, "MATLAB/Simulink based design & dovelopment of 5kW solar PV-grid connected power system; trends and challenges," in 2017 International Conference on Circuit, Power and Computing Technologies (ICCPCT), Apr. 2017, pp. 1–7, doi: 10.1109/ICCPCT.2017.8074214.
- [29] Z. Zeng, H. Li, S. Tang, H. Yang, and R. Zhao, "Multi-objective control of multi-functional grid-connected inverter for renewable energy integration and power quality service," *IET Power Electronics*, vol. 9, no. 4, pp. 761–770, Mar. 2016, doi: 10.1049/ietpel 2015 0317
- Q. Xu, F. Ma, A. Luo, Z. He, and H. Xiao, "Analysis and control of M3C-based UPQC for power quality improvement in medium/high-voltage power grid," *IEEE Transactions on Power Electronics*, vol. 31, no. 12, pp. 8182–8194, Dec. 2016, doi: 10.1109/TPEL.2016.2520586.
- [31] M. A. Rodriguez-Guerrero, A. Y. Jaen-Cuellar, R. D. Carranza-Lopez-Padilla, R. A. Osornio-Rios, G. Herrera-Ruiz, and R. de J. Romero-Troncoso, "Hybrid approach based on GA and PSO for parameter estimation of a full power quality disturbance parameterized model," *IEEE Transactions on Industrial Informatics*, vol. 14, no. 3, pp. 1016–1028, Mar. 2018, doi: 10.1109/TII.2017.2743762.
- [32] U. Subudhi and S. Dash, "Detection and classification of power quality disturbances using GWO ELM," *Journal of Industrial Information Integration*, vol. 22, Jun. 2021, doi: 10.1016/j.jii.2021.100204.

## **BIOGRAPHIES OF AUTHORS**



Ashish Ranjan © S B.Tech. in Electrical & Electronics Engineering from School of Engineering, Cochin University of Science and Technology, Kochi, Kerala and M.Tech. in Power System from Delhi Technological University, Delhi. Currently, he is pursuing his PhD from NIT Patna. His area of research includes Power Electronics and FACTs Devices, renewable energy sources and high voltage power transmission, Electrical protection. He can be contacted at email: ashishr.phd19.ee@nitp.ac.in.



Jayanti Chaudhary (D) SS did B.Sc. Engineering in Electrical Engineering Department of M.I.T Muzaffarpur, MTech in Power Electronics and Electrical Machines and drives from I.I.T Delhi and Ph.D. from Electrical Engineering Department of N.I.T Patna. She is currently an assistant professor in EED of NIT Patna. Her research area is power electronics and its applications in FACTS, Industrial drives and Controls and, Active Filters. She can be contacted at email: Jayanti@nitp.ac.in.